Fiber Optical Tweezers for Applying and Measuring Forces in a 3D Solid Compartment

Chaoyang Ti, Minh-Tri Ho Thanh, Yao Shen,
Qi Wen and Yuxiang Liu

Additional information is available at the end of the chapter

http://dx.doi.org/10.5772/intechopen.71757

Abstract

We developed an inclined dual fiber optical tweezers (DFOTs) for simultaneous force application and measurements in a 3D hydrogel matrix. The inclined DFOTs provide a potential solution for cell mechanics study in a three-dimensional matrix.

Keywords: fiber optics, optical trapping and manipulation, optical tweezers, mechanical properties measurement, cell mechanics study

1. Introduction

Optical tweezers (OTs) have been widely used in manipulating micro- or nanoscale particles and measuring nanometer-scale displacements since Arthur Ashkin pioneered the field in the early 1970s [1]. OTs have enabled significant advances in a range of applications in in biological and physical researches, such as the study of the motion of individual motor proteins [2, 3], rheology measurements of cell cytoskeleton response to external stimuli [4, 5], and mechanical properties of polymers [6]. Conventional OTs rely on high-numerical-aperture objective lenses. The intrinsic limitations, such as being bulky, expensive, the lack of flexibility, and the requirement of substrate transparency, significantly hinder the application of conventional OTs in emerging biophysical topics such as cellular mechanics in a three-dimensional (3D) environment.

Both mechanical forces generated by cells [7] and external forces applied on cells [8] have been shown not only to determine cell behaviors, but also to regulate biological development such as proliferation [9] and differentiation [10]. Currently, most of cellular force characterization has been carried out on deformable and homogeneous cell substrates [11, 12]. Cellular traction force can be backed out by measuring the local deformation of substrate. These techniques are also called traction force microscopy (TFM). Polyacrylamide gel is one of the most commonly used substrates for TFM. Its linear elastic properties lie in the range of deformation induced by single cells. Therefore, Polyacrylamide gel has been wildly used to measure cellular forces based on the substrate deformation during the cell attachment and migration [7], to investigate cell behaviors under various conditions of extracellular matrix (ECM) (e.g., by varying substrate stiffness) [13, 14], and to study traction forces of cells fully encapsulated in an elastic gel matrix [15].

In TFM, the mechanical properties of the substrate have to be pre-characterized in order to obtain the cell traction forces from the measured deformation field. Generally, local mechanical properties of the substrates, such as polyacrylamide gel, is measured by using atomic force microscopy (AFM) [16, 17]. However, the AFM based microrheology measurements require physical contact, and the resolution of lateral force measurements is limited. Micropost arrays [18] are an alternative substrate structure that has been used to replace polyacrylamide gel. However, these techniques cannot measure cellular forces in 3D compartments. Measurements of cellular traction forces in 3D compartments are important, since the behaviors of cells are different in a native environment, which is always inhomogeneous and 3D, compared to a 2D substrate [19]. Legant et al. quantified traction forces of cells embedded in a 3D hydrogel matrices by tracking a large number of fluorescent beads around the cells [15]. However, it is challenging to provide real-time measurements, since the post-process is time-consuming. In addition, a homogeneous elastic medium is required in order to back out the cellular forces for all the techniques mentioned above.

In this chapter, we demonstrate a versatile and flexible fiber optical trapping system, namely the inclined dual fiber optical tweezers (DFOTs) [20, 21], for measuring forces on and applying forces to particles embedded in a 3D compartment, without requiring any physical contact with the particles. It can reach anywhere in a liquid medium and does not require the substrate transparency. The trap can work with particles high above the substrate or those encapsulated inside a solid 3D compartment but close to the surface. Since the inclined DFOTs create traps without relying on the bulky objective lens, they have great potential to be miniaturized and integrated.

We demonstrate that the maximum force provided by the inclined DFOTs is comparable with that of conventional optical tweezers. For example, in our experiment with the inclined DFOTs, we obtained an optical force of ~20 pN on a 4.63 μm silica bead when an optical power at each fiber tip was 100 mW. By comparison, the maximum optical trapping forces provided by the conventional OTs is around 10 pN per 100 mW for micrometer-sized beads [22]. Moreover, compared with conventional OTs, the inclined DFOTs could allow a higher optical trapping power before possible photodamage occurs to a trapped cell. This is due to the following two reasons. (1) The optical power is distributed over a large area of cell surfaces from both sides of the inclined DFOTs, and hence the intensity is lower on the cell. By comparison, conventional optical tweezers focusing all the power in a sub-micron spot, resulting in a higher intensity and likelihood of photodamage with the same power. (2) The optical beam size in the inclined DFOTs is around 30 μm at the trap position (beam intersection), so the effective trapping power illuminated on a 5 μm bead is much less than the power emitted from the fiber tip.

In this work, the calibration of the optical trapping spring constant was carried out on microscale silica beads in water as well as those embedded in 3D polyacrylamide gel compartments. In addition, the *in-situ* characterization of polyacrylamide gel stiffness was performed by optical trapping measurements, and the results are in agreement with AFM measurements. Since there is no requirement for the polyacrylamide gel to be homogeneous in the optical trapping measurements, our results imply that the inclined DFOTs can be potentially used to characterize local mechanical properties of a 3D inhomogeneous, nonlinear medium. In addition, by varying the optical power of the inclined DFOTs, we can change the effective spring constant on the particles encapsulated in a polyacrylamide gel compartment. These results indicate that the inclined DFOTs can be used as a powerful tool to apply forces to biologic samples, for example cells, and to measure their responses simultaneously in a native 3D inhomogeneous environment.

2. Methodology

2.1. System setup and working principles

In the optical trap, optical forces arise from the momentum transfer during the scattering or refraction of incident photons [23]. When a dielectric particle, with a refractive index higher than the surrounding medium, is illuminated by a light beam, it will change the direction of light beam and in turn experience a force that is described as the sum of two components: a scattering force directed along the light beam and a gradient force pointing to the region of maximum light intensity. Traditionally, an optical trap is created by focusing a single laser beam with a high numerical aperture objective, which is called objective based OTs. Unlike objective based OTs, the inclined DFOTs create traps based on two inclined optical beams that can apply two sets of gradient forces and scattering forces, as shown **Figure 1(a)**. Once the four optical forces balance with all other forces that the particle is subject to, such as viscous drag force and gravity, a 3D optical trap can be successfully created.

The setup of the inclined DFOTs was based on our previous work [20, 24, 25]. Briefly, we set up the inclined DFOTs on an inverted microscope platform. Each fiber was mounted on a common board and was aligned with respect to the other via a miniature 3D translational stage and a micro 1D rotational stage, as shown in **Figure 1(a)**. The fiber inclination angle and fiber separation was also controlled by adjusting these stages. The position of the optical trap was then adjusted by manipulating the common board via another 3D translational stage.

The measurement setup is shown in **Figure 1(b)**. Light from a 980 nm laser diode (AC 1405-0400-0974-SM-500, Eques) was split into two lensed fibers (Nanonics Imaging, Ltd) through

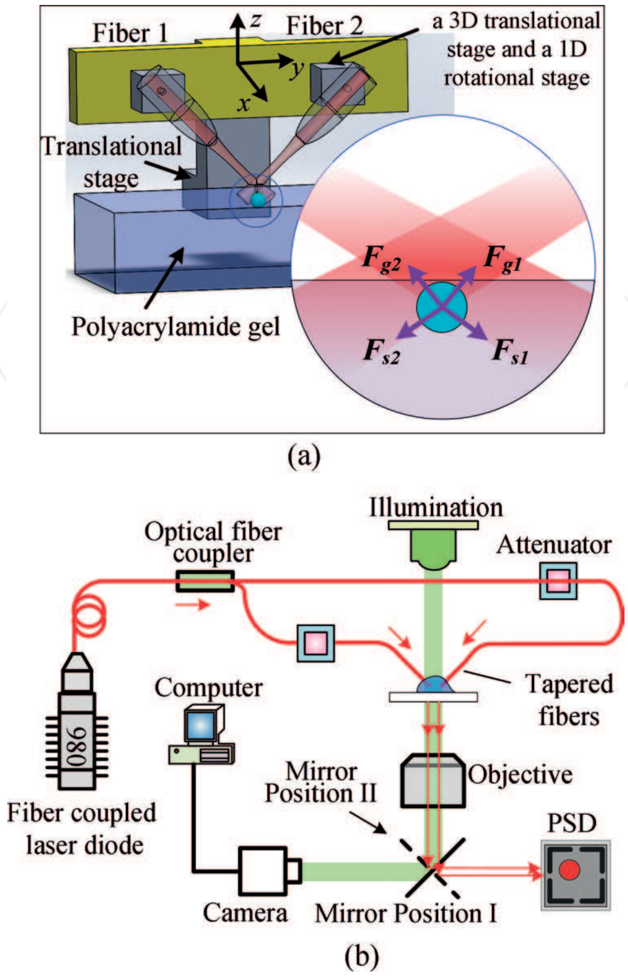

Figure 1. (a) Working principles and the setup schematic of the inclined DFOTs. The inclined DFOTs can be moved by a single translational stage that controls the position of the aluminum plate (top rectangular board in the figure). (b) Schematic of the measurement setup of the inclined DFOTs. F_s = scattering force; F_g = gradient force.

a 3 dB coupler. The equalized optical power outputs from the two lensed fiber ends were ensured by attenuators. When a micro silica bead in water or in polyacrylamide gel was trapped, the light scattered by the bead was collected by an objective lens and detected by a position-sensitive detector (PSD) (DL100-7-PCBA3, First Sensor), which enabled precision measurements of bead displacements in the x, y, and z directions with a nanometer resolution. All the fibers in the system are single mode at the wavelength of 980 nm.

2.2. Power spectrum calibration of optical spring constant

In this paper, calibration of the optical tweezers was accomplished by the power spectrum analysis method [26]. In the power spectrum analysis, the motion of a particle was confined by the restoring "spring" forces provided by the optical trap as well as the surrounding medium (such as the polyacrylamide gel) and can be expressed by [26]

$$m\ddot{x}(t) + \gamma\,\dot{x}(t) + k_x\,x(t) = \left(2\,k_B\,T\,\gamma_0\right)^{1/2}\eta(t), \tag{1}$$

and the one-sided power spectrum of the particle displacement can be expressed as [23, 25]

$$S_{xx}(f) = \frac{k_B T}{\pi^2 \gamma (f_0^2 + f^2)}, \tag{2}$$

where T is the absolute temperature, k_B is the Boltzmann's constant, γ represents the hydrodynamic drag coefficient ($\gamma = 6\pi\eta a$ for the Stokes drag on a spherical particle with a radius of a and a medium viscosity of η), and f_0 stands for the corner frequency that is related to the trapping spring constant k by

$$k = 2\pi\gamma f_0. \tag{3}$$

In our experiments, the motion of the trapped particle was detected by the PSD output signals that were recorded in a period of 5 seconds at a sampling rate of 50 kHz. Its power spectra were obtained by complex Fourier transform of the PSD signals [26]. The sampling rate in the experiment was much larger than the measured corner frequency, which in our case is tens of Hz. The exponential distributed power spectrum data were then blocked and transformed to Gaussian distribution, which was used to follow the least square curve fitting. Being fitted to a Lorentzian in Eq. (1) with a frequency range of 10–800 Hz, the blocked power spectra provided the calibration results of the spring constants following Eq. (2). The calibration of the spring constant of the inclined DFOTs does not require excitation of particle motion at any specific frequencies. The calibration is passive and relies only on monitoring the confined Brownian motion of trapped particle. Therefore, the inclined DFOTs can be used for *in-situ* and real-time measurements.

2.3. Experimental measurements in water

We first investigated the dependence of the spring constant of the inclined DFOTs on the optical power in water, which allowed us to better characterize the inclined DFOTs. The results obtained in water set the base for polyacrylamide gel characterization that was described in Section 2.4. Silica beads (Bangs Laboratories, Inc.) with a density of 2.0 g/cm^3 and a diameter of 4.63 μm were used in all experiments. A diluted silica bead solution, with a ratio of deionized (DI) water to original bead solution (10.2%, 0.5 g in weight) at 6000:1 was ultrasonicated in order to reverse bead aggregation. One drop of diluted bead solution (~0.2 ml) was added on a coverglass, where the trapping experiment was carried out. In order to reduce the sidewall effects, we accomplished the optical trap calibration with beads 3D trapped around 35 μm above the coverslip [22].

2.4. Experiment measurements in polyacrylamide gel

In this experiment, the inclined DFOTs were used to apply tunable forces on a bead embedded in the polyacrylamide gel without any physical contact. In the meantime, the resultant motion of the bead was monitored and measured by the PSD to enable spring constant calibration of both the optical trap and the polyacrylamide gel. By varying the optical power, the optical force provide by the inclined DFOTs was readily tuned, which enables the calibration of the effective spring constant of the hydrogel.

2.4.1. Polyacrylamide gel sample preparation

Polyacrylamide gels were fabricated on 25×25 mm^2 coverslips. In all the experiments, we prepared the polyacrylamide gel solution with the desired concentration of 5% acrylamide and 0.04% bisacrylamide in a pH 8.2 HEPES buffer. By adding 3 μl tetramethylethylenediamine (TEMED) and 10 μl of 10% ammonium persulfate (APS) solution for each 1 ml of polyacrylamide gel solution, we can initiate the polymerization process. The polyacrylamide gel solution was then quickly transferred to a glutaraldehyde-activated coverslip and covered by a second plasma-cleaned coverslip, on which dried silica beads with a diameter of 4.63 μm were attached previously. A polymerized polyacrylamide gel with a desired thickness of ~ 50 μm was achieved by controlling the volume of polyacrylamide gel solution on each coverslip to be 30 μl. The gelation was complete after curing the gel solution for 15 minutes at the room temperature. We obtained the polyacrylamide gel sample with silica beads embedded on the its top after peeling off the second coverslip. Due to the deformation of the polyacrylamide gel during the polymerization process, not all the beads are on the polyacrylamide gel surface. Beads close to the surface of the polyacrylamide gel were selected for the optical trapping experiments.

2.4.2. Optical trapping experiment of polyacrylamide gel calibration

The optical trapping experiment of polyacrylamide gel calibration was carried out by analyzing the confined motion of the bead, which resulted from the confinement effects of both the optical trap and the polyacrylamide gel. A bead close to the polyacrylamide gel top surface was first identified, and the inclined DFOTs were moved to this pre-identified location so that the bead was in the optical trap. The power spectrum measurements enabled the calibration of an effective spring constant. The tunable optical spring constant was achieved by varying the optical power, which allowed the polyacrylamide gel stiffness to be calibrated.

2.4.3. AFM measurements of polyacrylamide gel moduli

In this work, AFM [16, 17] was used to characterize local viscoelastic properties of polyacrylamide gel around the bead that was studied in the inclined DFOTs. An Asylum Research MFP3D-BIO AFM (Asylum Research, CA) was used for the measurements. Briefly, The AFM cantilever was first moved to the location above the polyacrylamide gel top surface around the selected bead that was studied by the inclined DFOTs. The cantilever was then lowered down to create an approximate 2 μm indentation in the gel. A small oscillating indentation at the tip was generated by driving the cantilever sinusoidally with an amplitude of 25 nm and a frequency $f = 10$ Hz. The gel elastic modulus (E') and the viscous modulus (E''), which are also referred to as the storage and loss moduli, respectively, were measured based on the cantilever force and indentation. The experimentally measured E' and E'' are 1469.9 ± 555.9 Pa and 533.2 ± 243.4 Pa, respectively (see Section 3.2.2). The viscosity of the polyacrylamide gel was calculated using $\eta = E''/2\pi f$.

http://dx.doi.org/10.5772/intechopen.71757

3. Experimental results and discussion

3.1. Experimental results in DI water and discussion

In this section, we will demonstrate the capability of the inclined DFOTS to apply and measure 3D forces in aqueous environments.

3.1.1. 3D trapping of yeast cells in DI water

3D trapping of silica beads with the inclined DFOTs was demonstrated in our previous work [20, 24, 25]. Here, we show that the inclined DFOTs are also applicable to 3D trapping of biological samples. In this experiment, the inclined DFOTs were used to trap and manipulate a living yeast cell in all three dimensions in DI water, as shown in **Figure 2**. The trapped yeast cell was moved via controlling the aluminum board (see yellow block in **Figure 1(a)**) by a single 3D stage (not shown in **Figure 1(a)**). The maximum moving speed of the trapped cells was dependent on the optical power. For example, the maximum moving speed was measured to be around 20 μm/s before the yeast cells escaped from the trap, when the optical power is 6.8 mW from each fiber. Manipulating the 3D positions of living cells bestows on the inclined DFOTs the capability of relocation and assembly of living biological particles with micrometer size.

3.1.2. Optical trapping spring constant calibration in water

Silica beads with the size of 4.63 μm were used to carry out the calibration of the trapping spring constant. The uniformity in shape and material properties allows silica beads to serve as appropriate samples for evaluating the capability of the inclined DFOTs.

The optical trapping spring constant can be measured by the bead displacement power spectrum when a silica bead is trapped in three dimensions in water. **Figure 3(a)** and **(c)** show the typical power spectrum data of a bead trapped in water in the x and y axes, respectively. The corresponding corner frequencies obtained by fitting the blocked power spectra to Lorentzian are 86.0 ± 3.3 Hz in the x axis (**Figure 3(a)**) and 74.4 ± 3.1 Hz in the y axis (**Figure 3(c)**). We notice that the spring constants in the x and y directions are different, which are mainly due to different optical field distributions along the two directions, as shown in **Figure 1(a)**. The linear dependence of optical spring constant on optical power along the x and y directions is shown in **Figure 3(b)** and **(d)**, respectively. The maximum power used in the experiment is 120 mw and the corresponding spring constants of the inclined DFOTs are 22.1 ± 1.0 pN/μm and 21.5 ± 0.9 pN/μm in the x and y directions, respectively. The tunable optical forces can be determined by measuring the displacement of the trapped particle. According our previous results [20], the linear range of the force-displacement relationship is around −1 to 1 μm, and the maximum bead displacement in the inclined DFOTs is around 2 μm before it escapes from the trap. When the bead displacements is between 1 and 2 μm, the trap is not stable and the bead may easily escape.

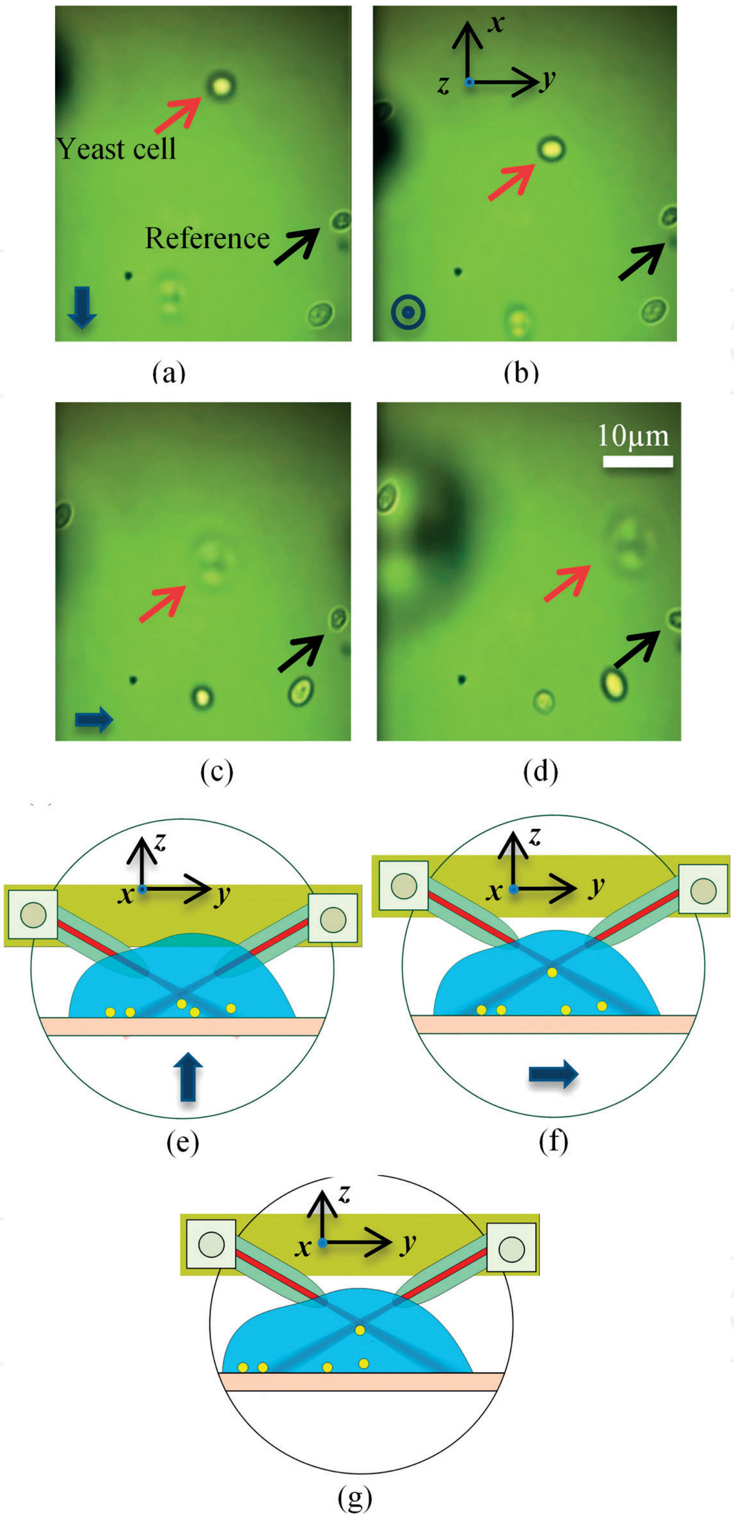

Figure 2. 3D trapping of living yeast cells with the inclined DFOTs in water [24, 25]. (a–d) Microscope images of trapping a yeast cell. The yeast cell was trapped (a) and manipulated in the (b) −*x* direction, followed by (c) +*z* and (d) +*y* directions. The corresponding next movements of the optical trap are shown in the lower left corners of (a–c) and at the bottom of (e–f). The upper arrows represent the trapped yeast cell, and the lower arrows are the reference yeast cell. (e–g) Schematics showing the positions of the fibers and trapped beads in (b–d), respectively. The shadow shown on the left-hand side of (a–d) is the trapped fiber tip. The optical power from each fiber taper was 6.8 mW.

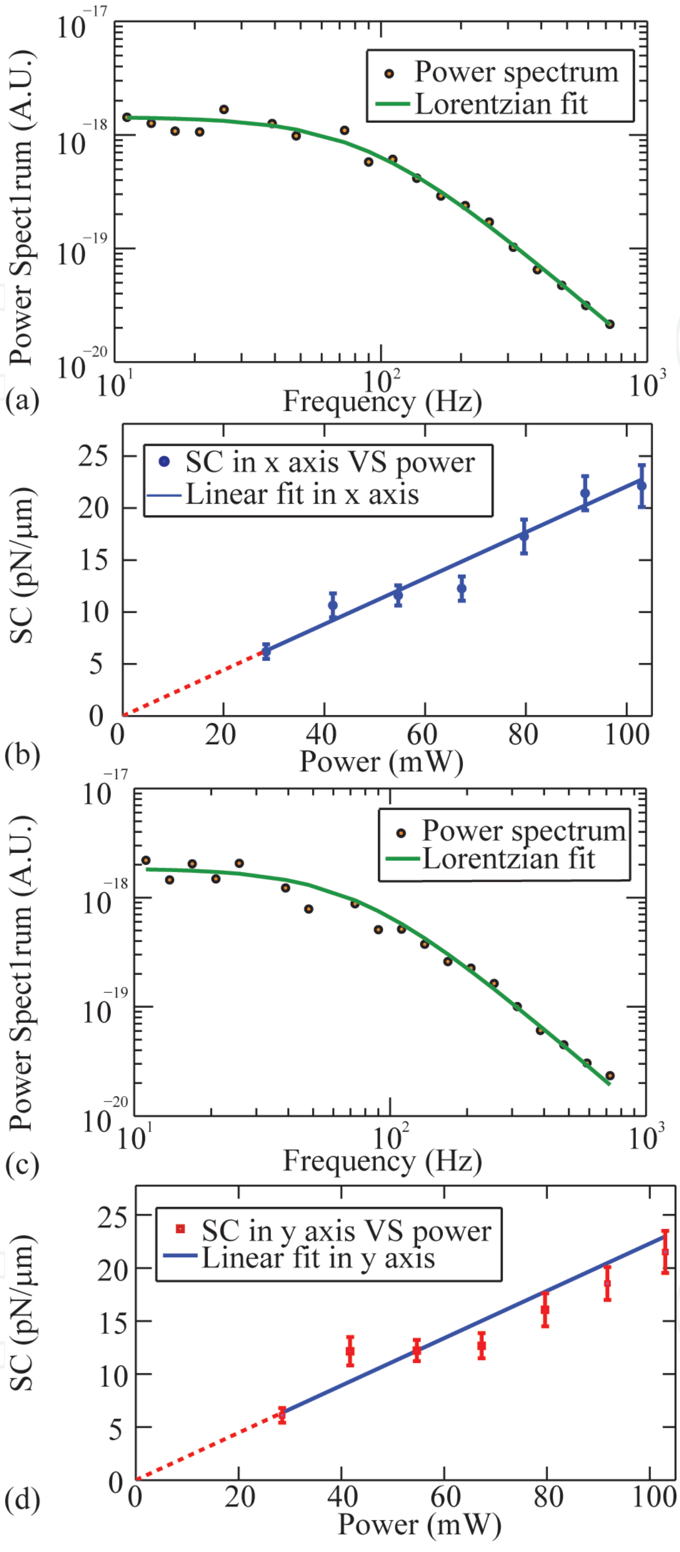

Figure 3. Experimentally measured power spectrum data of a 4.63 μm bead trapped in water (hollow circles) and Lorentzian fitting (solid curves) at 91.76 mW in the (a) x and (c) y directions. Optical trapping spring constant as a function of optical power in the (b) x and (d) y directions. The linear fitting (solid line) of spring constant on optical power passes point (0, 0). The extension is the dashed line. The optical power drawn in the figure is the power emitted by each fiber. SC stands for spring constant.

It is noted that the optical force can be calculated by multiplying optical trapping spring constant by the bead displacement. The results in **Figure 3(b)** and **(d)** indicate that the inclined DFOTs can provide forces ranging from sub-pN to tens of pN. It implies that the inclined DFOTs can be used to measure cellular forces, since various cellular forces lie in this range, such as those generated by neural growth cone [27] and by a single actin filament [28]. Compared with the force sensing range of AFM, which is in the range of 10 pN to 100 nN [29], the force range of inclined DFOTs may extend the range of the biological applications and measurable quantities that may be challenging for AFM.

The error bars in **Figure 3(b)** and **(d)** are the 95% confidence interval ranges of the Lorentzian curve fitting. It can be seen that there is a linear relationship between the spring constant and the optical power in both x and y directions. The results in water confirm that the optical force can be well characterized, which enables the inclined DFOTs to exert controlled optical forces as well as measurements of external forces on the trapped particles.

There are data points in **Figure 3(b)** and **(d)** scattering around the fitted linear curve. This may be that the z-dimensional equilibrium position (see **Figure 1(a)**) of the trapped bead is dependent on the optical power. It could introduce a nonlinearity between the spring constant and optical power. In addition to the errors of the Lorentzian fitting, other sources of the uncertainties include electronic noise, external noise, as well as errors of the bead diameter.

3.2. Experimental measurements of polyacrylamide gel and discussion

3.2.1. Experimental results measured by inclined DFOTs

In the experiments, the effective spring constant was changed by tuning the optical power. We obtained the dependence of effective spring constant on power in the y direction, as shown in **Figure 4(b)**. Each single data point in **Figure 4(b)** is acquired from the Lorentzian fitting of a set of power spectrum data at a fixed power as described in Section 2.2. A typical set of power spectrum data is shown in **Figure 4(a)**. It is seen that there exists a linear relationship between the effective spring constant and the optical power, as shown in **Figure 4(b)**. In the experiment, since the effective spring constant is attributed to both the optical trapping and the polyacrylamide gel, the intrinsic stiffness of the polyacrylamide gel with no laser illumination can be obtained to be 0.012 ± 0.005 N/m, which is based on the intersect of the fitted curve with the vertical axis. The error bar is determined by the standard deviation of 4 independent measurements. We show one of the spring constant-power curves in **Figure 4(b)**. This enables the inclined DFOTs to characterize the mechanical properties of solid media *in-situ*. Optical forces on embedded beads can be calculated by measuring the bead displacement once the equivalent spring constant of polyacrylamide gel is characterized.

Since the calibration of the material equivalent spring constant is accomplished by monitoring the bead confined Brownian motion, the inclined DFOTs can used to measure the stiffness of nonlinear materials. We estimate that the effective root-mean-square displacement of the Brownian motion is around 0.6 nm for a bead embedded in a material with an equivalent spring constant of 0.012 N/m at the room temperature. Most of the materials can be considered to be linear and uniform in such a small range as 0.6 nm, so the material equivalent

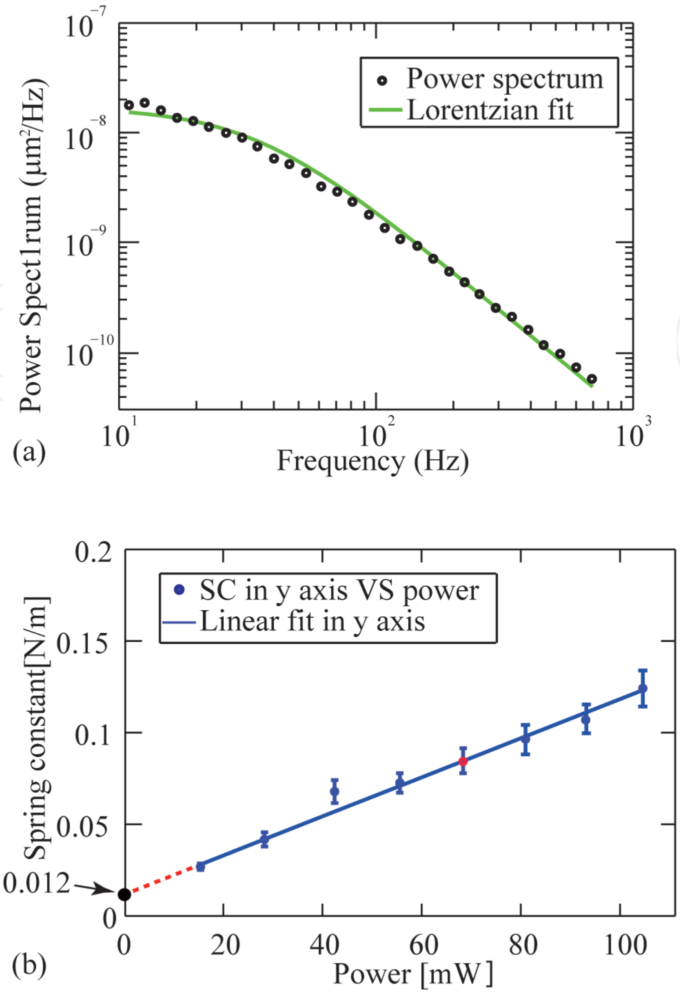

Figure 4. (a) A typical set of experimental power spectrum data fitted by a Lorentzian in the polyacrylamide gel at the power of 67.0 mW, which corresponds to the fifth data point in (b). (b) The effective y-axis (see **Figure 1(a)**) spring constant as a function of optical power for a bead embedded in the polyacrylamide gel. The intersection with the vertical axis of 0.012 N/m indicates the polyacrylamide gel stiffness. SC stands for spring constant.

spring constant can be calibrated *in situ*. As a result, unlike other measurements where material linearity is important, such as traction force microscopy, the optical trapping measurement of the material properties (and hence the forces) is not dependent on the linearity or homogeneity of the materials.

In addition, unlike traditional AFM measurements which require physical contact, no physical contact is needed for the inclined DFOTs. This enables the inclined DFOTs to work with particles embedded in 3D matrices. Although the traction force microscopy has been demonstrated in a homogenous 3D medium, it is still challenging to realize real-time measurements due to the requirement of tracking large numbers of fluorescent beads [15]. By comparison, the inclined DFOTs have a potential to provide a real-time, versatile, and non-invasive way to measure the material properties inside a 3D heterogeneous and nonlinear medium.

It is noted that laser illumination can affect the mechanical properties of polyacrylamide gel in the experiment. For example, under laser illumination, local temperature changes originating from optical absorption of the trapped particle can change the surrounding medium viscosity [30]. The polyacrylamide gel stiffness has also been observed to change under localized laser illumination [31, 32]. Moreover, polyacrylamide gel mechanical integrity can also be changed [31] due to the nature of polyacrylamide gel swelling. In addition, the effective polyacrylamide gel property may be influenced due to the imperfect contact condition at the interface between bead and surrounding polyacrylamide gel. In our experiments, we noticed differences in data obtained in water and polyacrylamide gel, mainly in the slope of spring constant-power curve, shown in **Figures 3(b)**, **(d)**, and **4(b)**. Although we do not fully understand how the polyacrylamide gel has been changed by laser illumination, we observed the linear dependence of corner frequencies on optical power, because the spring constant-power data in polyacrylamide gel can be well fitted by linear functions. According to the repeatability of our optical trapping measurements of the polyacrylamide gel stiffness, we believe the laser-induced polyacrylamide gel changes are reversible. As a result, the capability of the inclined DFOTs to measure the intrinsic polyacrylamide gel stiffness will not be influenced by the laser induced polyacrylamide gel changes, since the measurement of the intrinsic polyacrylamide gel stiffness with the inclined DFOTs is determined by the intersect of the linear fitting curve on the vertical axis.

3.2.2. Experimental results measured by AFM

AFM based microrheology measurements [16, 17] were also used to characterize the local viscoelasticity of polyacrylamide gel. In this work, AFM was used to serve as a reference to verify the inclined DFOTs measurements. To ensure the statistical measurements, we characterized the viscoelastic properties of polyacrylamide gel at 19 different locations around the bead of interest. The typical AFM force and indentation curves, shown in **Figure 5(a)**, can be fitted by sinusoidal function to remove noise. **Figure 5(b)** plots the force as a function of indentation. Its raw data and the corresponding fitted data is shown as the blue and red curves, respectively. The hysteresis in **Figure 5(b)** indicates the viscoelasticity of polyacrylamide gel, which can be used to back out the elastic and viscous moduli. Following the analysis method in Ref. [16], the elastic and viscous moduli of the polyacrylamide gel can be calculated and obtained to be 1469.9 ± 555.9 Pa and 533.2 ± 243.4 Pa, respectively. The mean values and standard deviations of the moduli were determined by 19 independent measurements. As a result, based on the viscous moduli of the polyacrylamide gel, we obtained its viscosity to be 8.5 ± 3.9 Pa · s.

3.2.3. Comparison of the inclined DFOTs and AFM results

In the experiments, the optical trapping experiments measure the effective spring constants (with a unit of N/m) on a silica bead, which is dependent on bead size, the bead location, and the elastic modulus of polyacrylamide gel. However, AFM measures the elastic modulus (with a unit of Pa). To compare them, we used the commercial finite element analysis software (COMSOL) to calculate the spring constant on a bead embedded in the top surface of polyacrylamide gel using the elastic modulus measured from the AFM experiments. We then compared the spring constant obtained by the inclined DFOTs measurements with that calculated from COMSOL.

http://dx.doi.org/10.5772/intechopen.71757

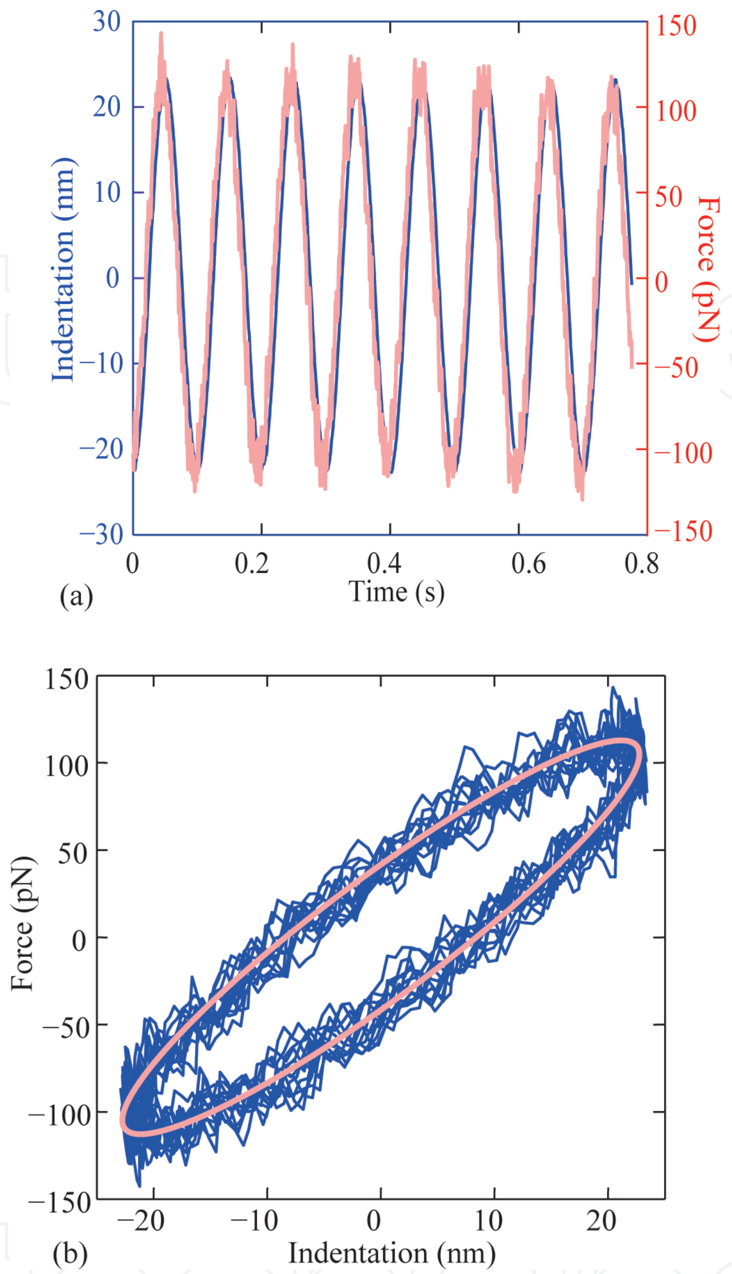

Figure 5. AFM microrheology measurements of the polyacrylamide gel. (a) A typical measurement of the sinusoidal force ("thick" curve) and indentation ("thin" curve) as functions of time. (b) Force as a function of indentation. The "thin" curve is obtained from the raw data in (a), and the smooth "thick" curve is from the sinusoidal fitting of the data in (a).

We use the Kelvin-Voigt model to describe the viscoelasticity of polyacrylamide gel in the simulation. By applying a 20 nN static body force applied parallel to the polyacrylamide gel surface, we obtain the displacement of a silica bead embedded in the polyacrylamide. The polyacrylamide gel stiffness is then calculated based on the resultant bead displacement and the applied force.

According to the procedures of polyacrylamide gel preparation, the beads selected for optical trapping measurements were always close to the top surface of polyacrylamide gel. However, due to the polyacrylamide gel deformation during the polymerization process, it was challenging

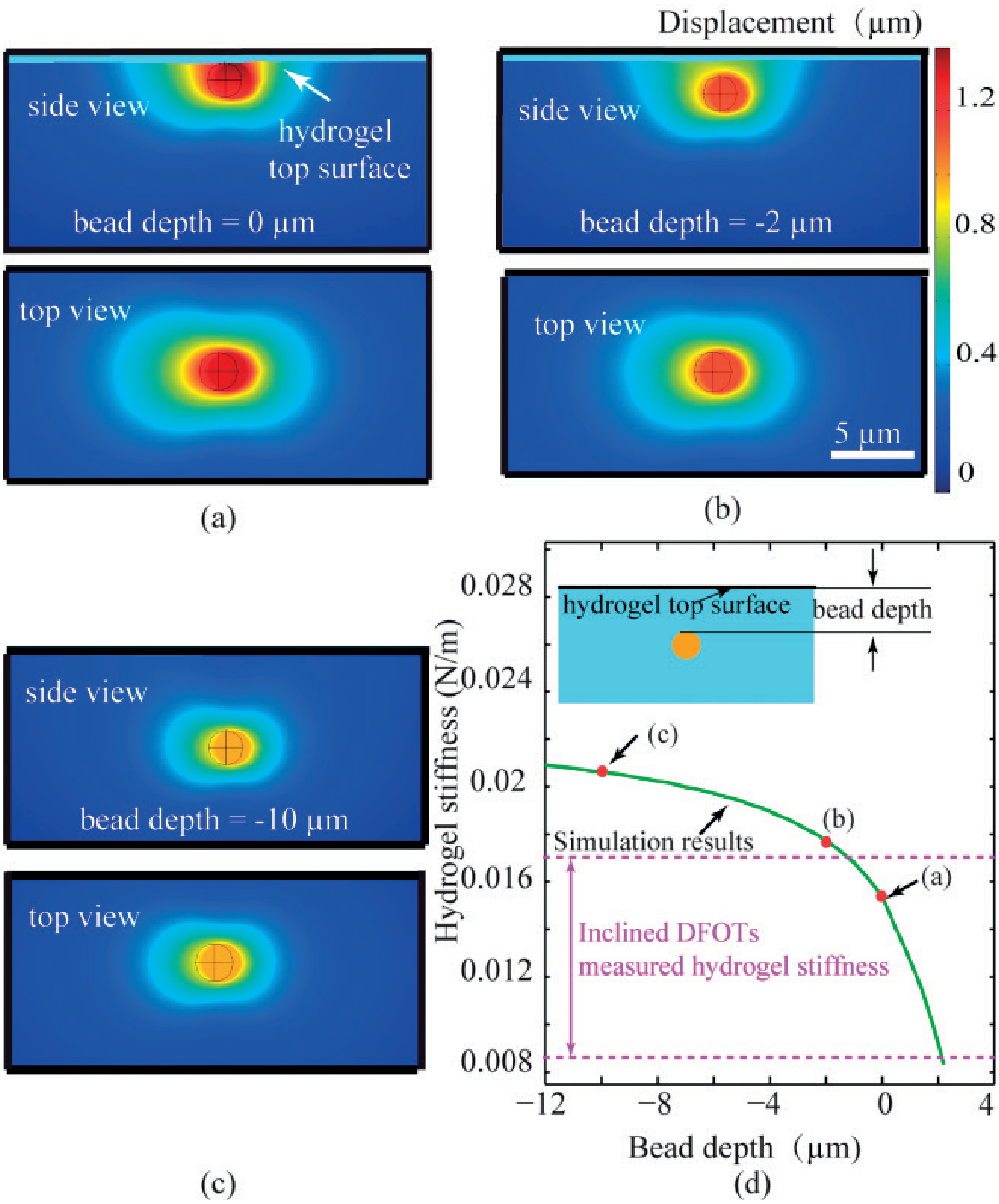

Figure 6. (a–c) COMSOL calculated the displacement field of a silica bead embedded in polyacrylamide gel when the bead depth is (a) 0, (b) −2 μm, and (c) −10 μm. The bead depth is defined to be 0 when the bead top surface is flush with the polyacrylamide gel top surface. The top and bottom figures are the side and top views, respectively. The total thickness of polyacrylamide gel used in the simulation is 50 μm. (d) Calculated dependence of the polyacrylamide gel stiffness on the bead depth based on simulation results. The three data points correspond to the results shown in (a–c), respectively. The inclined DFOTs measurements are also shown for comparison (two dashed lines). Inset: definition of bead depth.

to determine the precise position of the bead with respect to the polyacrylamide gel top surface. Therefore, it was important to investigate the influence of the polyacrylamide gel stiffness on the depth of the bead in the simulation. In the simulation, we obtain the polyacrylamide gel stiffness shown in **Figure 6(a)–(c)** to be 0.0154 N/m, 0.0177 N/m, and 0.0206 N/m, respectively. It is noted that the deeper the bead, the larger the stiffness. In addition, due to the weaker polyacrylamide gels surface effects, the rate of change of the stiffness is smaller with deeper bead positions. The polyacrylamide gel displacement field is not influenced much by the surface when the bead is far away from the polyacrylamide gel surface, as shown in **Figure 6(c)**. When the bead is deeper than 10 μm from the surface, the stiffness variation becomes small, as shown in **Figure 6(d)**.

According to the simulation results shown in **Figure 6(d)**, we can see that the optical trapping measurement of polyacrylamide gel stiffness agrees with the simulation results based on AFM measurements when the bead top surface is in the range from −1 to 2 μm above the polyacrylamide gel surface. This proves that the inclined DFOTs can be a reliable tool to realize *in-situ*, non-invasive characterization of local material properties and forces in a 3D medium. In addition, since the spring constant of optical trapping is dependent on the optical restoring force applied on the embedded bead, we can vary the spring constant by tuning optical power. It demonstrates the capability of the inclined DFOTs to apply tunable forces in 3D compartments.

The ability of simultaneously applying and measuring forces enables the inclined DFOTs to be a potential tool for cell mechanics study in 3D compartments. The spring constant measurements bestows upon the inclined DFOTs capable of directly measuring forces on the bead if the displacement is monitored.

4. Conclusion

In this chapter, we show the inclined dual fiber optical tweezers (DFOTs) can be used for simultaneous applications and measurements of optical forces on particles in water and those in a 3D polyacrylamide gel compartment. Moreover, we demonstrate *in-situ* characterization of the polyacrylamide gel stiffness by the optical trapping measurements. The measured polyacrylamide gel stiffness agrees with finite element method (FEM) simulation results based on experimental AFM measurements. Since the optical trapping measurements do not require the medium to be mechanically homogeneous and linear, the inclined DFOTs can measure the mechanical properties of materials that are heterogeneous and nonlinear. The ability of simultaneous applying and measuring optical forces in a 3D compartment enables the inclined DFOTs to be a versatile tool that can be potentially useful for biomechanics and mechanobiology study.

Acknowledgements

This research is supported by the National Science Foundation under Grant No. CBET-1403257.

Author details

Chaoyang Ti[1]*, Minh-Tri Ho Thanh[2], Yao Shen[1], Qi Wen[2] and Yuxiang Liu[1]

*Address all correspondence to: chaoyang@wpi.edu

1 Department of Mechanical Engineering, Worcester Polytechnic Institute, Worcester, MA, USA

2 Department of Physics, Worcester Polytechnic Institute, Worcester, MA, USA

References

[1] Ashkin A. Acceleration and trapping of particles by radiation pressure. Physical Review Letters. 1970;**24**:156

[2] Svoboda K, Schmidt CF, Schnapp BJ, Block SM. Direct observation of kinesin stepping by optical trapping interferometry. Nature. 1993;**365**:721-727

[3] Finer JT, Simmons RM, Spudich JA. Single myosin molecule mechanics: Piconewton forces and nanometre steps. Nature. 1994;**368**:113-119

[4] Fabry B, Maksym GN, Butler JP, Glogauer M, Navajas D, Fredberg JJ. Scaling the microrheology of living cells. Physical Review Letters. 2001;**87**:148102

[5] Fredberg J, Fabry B. The cytoskeleton as a soft glassy material. In: Mofrad MRK, Kamm RD, editors. Cytoskeletal Mechanics: Models and Measurements. Cambridge, NY: Cambridge University Press; 2006

[6] Grier DG. Optical tweezers in colloid and interface science. Current Opinion in Colloid & Interface Science. 1997;**2**:264-270

[7] Dembo M, Wang Y-L. Stresses at the cell-to-substrate interface during locomotion of fibroblasts. Biophysical Journal. 1999;**76**:2307-2316

[8] Hickory WB, Nanda R. Effect of tensile force magnitude on release of cranial suture cells into S phase. American Journal of Orthodontics & Dentofacial Orthopedics. 1987;**91**:328-334

[9] Chen CS, Mrksich M, Huang S, Whitesides GM, Ingber DE. Geometric control of cell life and death. Science. 1997;**276**:1425-1428

[10] Roskelley C, Desprez P, Bissell M. Extracellular matrix-dependent tissue-specific gene expression in mammary epithelial cells requires both physical and biochemical signal transduction. Proceedings of the National Academy of Sciences. 1994;**91**:12378-12382

[11] Harris AK, Wild P, Stopak D. Silicone rubber substrata: A new wrinkle in the study of cell locomotion. Science. 1980;**208**:177-179

[12] Schoen I, Pruitt BL, Vogel V. The yin-yang of rigidity sensing: How forces and mechanical properties regulate the cellular response to materials. Annual Review of Materials Research. 2013;**43**:589-618

[13] Pelham RJ, Wang Y-l. Cell locomotion and focal adhesions are regulated by substrate flexibility. Proceedings of the National Academy of Sciences. 1997;**94**:13661-13665

[14] Gray DS, Tien J, Chen CS. Repositioning of cells by mechanotaxis on surfaces with micropatterned Young's modulus. Journal of Biomedical Materials Research Part A. 2003;**66**:605-614

[15] Legant WR, Miller JS, Blakely BL, Cohen DM, Genin GM, Chen CS. Measurement of mechanical tractions exerted by cells in three-dimensional matrices. Nature Methods. 2010;**7**:969-971

[16] Mahaffy R, Park S, Gerde E, Käs J, Shih C. Quantitative analysis of the viscoelastic properties of thin regions of fibroblasts using atomic force microscopy. Biophysical Journal. 2004;**86**:1777-1793

[17] Thomas G, Burnham NA, Camesano TA, Wen Q. Measuring the mechanical properties of living cells using atomic force microscopy. JoVE (Journal of Visualized Experiments). 2013;**76**:e50497-e50497

[18] Du Roure O, Saez A, Buguin A, Austin RH, Chavrier P, Siberzan P, Ladoux B. Force mapping in epithelial cell migration. Proceedings of the National Academy of Sciences of the United States of America. 2005;**102**:2390-2395

[19] Cukierman E, Pankov R, Stevens DR, Yamada KM. Taking cell-matrix adhesions to the third dimension. Science. 2001;**294**:1708-1712

[20] Liu Y, Yu M. Investigation of inclined dual-fiber optical tweezers for 3D manipulation and force sensing. Optics Express. 2009;**17**:13624-13638

[21] Liu Y, Yu M. Multiple traps created with an inclined dual-fiber system. Optics Express. 2009;**17**:21680-21690

[22] Neuman KC, Block SM. Optical trapping. Review of Scientific Instruments. 2004;**75**:2787-2809

[23] Svoboda K, Block SM. Biological applications of optical forces. Annual Review of Biophysics and Biomolecular Structure. 1994;**23**:247-285

[24] Ti C, Thomas GM, Wen Q, Liu Y. Fiber optical tweezers for simultaneous force exertion and measurements in a 3D hydrogel compartment. In: Lasers and Electro-Optics (CLEO). Washington, DC: Optical Society of America; 2015;**79**:1-2. JW2A.79

[25] Ti C, Thomas GM, Ren Y, Zhang R, Wen Q, Liu Y. Fiber based optical tweezers for simultaneous in situ force exertion and measurements in a 3D polyacrylamide gel compartment. Biomedical Optics Express. 2015;**6**:2325-2336

[26] Berg-Sørensen K, Flyvbjerg H. Power spectrum analysis for optical tweezers. Review of Scientific Instruments. 2004;**75**:594-612

[27] Hällström W, Lexholm M, Suyatin DB, Hammarin G, Hessman D, Samuelson L, Montelius L, Kanje M, Prinz CN. Fifteen-piconewton force detection from neural growth cones using nanowire arrays. Nano Letters. 2010;**10**:782-787

[28] Ananthakrishnan R, Ehrlicher A. The forces behind cell movement. International Journal of Biological Sciences. 2007;**3**:303-317

[29] Rodriguez ML. Review on cell mechanics: Experimental and modeling approaches. Applied Mechanics Reviews. 2013;**65**:510-518

[30] Seol Y, Carpenter AE, Perkins TT. Gold nanoparticles: Enhanced optical trapping and sensitivity coupled with significant heating. Optics Letters. 2006;**31**:2429-2431

[31] Chan BP. Biomedical applications of photochemistry. Tissue Engineering Part B: Reviews. 2010;**16**:509-522

[32] Mosiewicz KA, Kolb L, Van Der Vlies AJ, Lutolf MP. Microscale patterning of hydrogel stiffness through light-triggered uncaging of thiols. Biomaterials Science. 2014;**2**:1640-1651